

RESEARCH ARTICLE | DECEMBER 14 2021

Evidence of the dominant production mechanism of ammonia in a hydrogen plasma with parts per million of nitrogen

J. Ellis ; D. Köpp; N. Lang; ... et. al



Appl. Phys. Lett. 119, 241601 (2021)

<https://doi.org/10.1063/5.0072534>



CrossMark

Articles You May Be Interested In

Cost per million BTU of solar heat, insulation, and conventional fuels

American Journal of Physics (July 1984)

Million frames per second infrared imaging system

Rev Sci Instrum (October 2000)

Part-per-million gas detection from long-baseline THz spectroscopy

Appl. Phys. Lett. (September 2004)



Time to get excited.
Lock-in Amplifiers – from DC to 8.5 GHz

[Find out more](#)



Evidence of the dominant production mechanism of ammonia in a hydrogen plasma with parts per million of nitrogen

Cite as: Appl. Phys. Lett. **119**, 241601 (2021); doi: [10.1063/5.0072534](https://doi.org/10.1063/5.0072534)

Submitted: 23 September 2021 · Accepted: 1 December 2021 ·

Published Online: 14 December 2021



View Online



Export Citation



CrossMark

J. Ellis,^{a)}  D. Köpp, N. Lang,  and J. H. van Helden^{a)} 

AFFILIATIONS

Leibniz Institute for Plasma Science and Technology (INP), Felix-Hausdorff-Str. 2, 17489 Greifswald, Germany

^{a)} Authors to whom correspondence should be addressed: james.ellis@inp-greifswald.de and jean-pierre.vanhelden@inp-greifswald.de

ABSTRACT

Absolute ground state atomic hydrogen densities were measured, by the utilization of two-photon absorption laser induced fluorescence, in a low-pressure electron cyclotron resonance plasma as a function of nitrogen admixtures—0 to 5000 ppm. At nitrogen admixtures of 1500 ppm and higher, the spectral distribution of the fluorescence changes from a single Gaussian to a double Gaussian distribution; this is due to a separate, nascent contribution arising from the photolysis of an ammonia molecule. At nitrogen admixtures of 5000 ppm, the nascent contribution becomes the dominant contribution at all investigated pressures. Thermal loading experiments were conducted by heating the chamber walls to different temperatures; this showed a decrease in the nascent contributions with increasing temperature. This is explained by considering how the temperature influences recombination coefficients, and from which, it can be stated that the Langmuir–Hinshelwood recombination mechanism is dominant over the Eley–Rideal mechanism.

© 2021 Author(s). All article content, except where otherwise noted, is licensed under a Creative Commons Attribution (CC BY) license (<http://creativecommons.org/licenses/by/4.0/>). <https://doi.org/10.1063/5.0072534>

Plasmas containing a mixture of hydrogen and nitrogen are used in a plethora of applications including plasma nitriding,^{1,2} impurity seeding for power dissipation in fusion reactors,^{3,4} astrophysical comparisons,⁵ thin film growth,⁶ and for their potential in generating ammonia for industrial applications.⁷ The formation of ammonia in H₂–N₂ plasmas is not quantitatively understood; however, it is widely accepted that production is dominated through plasma–surface interactions. The production mechanism is the progressive hydrogenation of nitrogen species⁸ in which atomic species at the wall undergo a series of recombination reactions through both the Langmuir–Hinshelwood (LH) and Eley–Rideal (ER) mechanisms.⁹ There are a number of previous studies on H₂–N₂ plasmas; however, these are mostly focused on larger admixtures with relatively large incremental steps. Significant work has been conducted by a number of authors to understand the complex chemical environment of H₂–N₂ plasmas.^{3,5,10–13} This study focuses exclusively on measuring atomic hydrogen densities, from two different contributions, and their relative changes with very small incremental steps in the nitrogen admixture. The low, and narrow, pressure range (3–7 Pa) used in this study allows the focus to shift from the volume of the plasma to the plasma–surface

interactions that are generally accepted as being of pivotal importance to the generation of ammonia. The partial fraction of N₂ was varied up to a maximum of 5000 ppm, but the pressures were kept constant in each case. The measured atomic hydrogen densities and nascent contribution, attributed to the creation of ammonia, are discussed in reference to the surfaces of the reactor vessel. Finally, these surfaces were heated to various temperatures, and a significant effect of this thermal loading was observed.

In this Letter, the significant role of impurity seeded nitrogen on an otherwise pure hydrogen plasma is presented. This is manifested by a significant production of ammonia that can be linked to a dissociation degree that is a factor of 500 higher for nitrogen as opposed to hydrogen. It is also shown that the dominant mechanism for the formation of ammonia must be the LH recombination mechanism.

Figure 1 shows the schematic representation of the beam line, reactor, and detection apparatus. The beam line allows the production of 205 nm radiation that is created through the combination of a frequency doubled Spectra Physics Quanta Ray Nd:YAG pump laser, with a pulse width of 6 ns, and a Sirah Precision Scan SL dye laser. The 615 nm red light from the dye laser then undergoes frequency

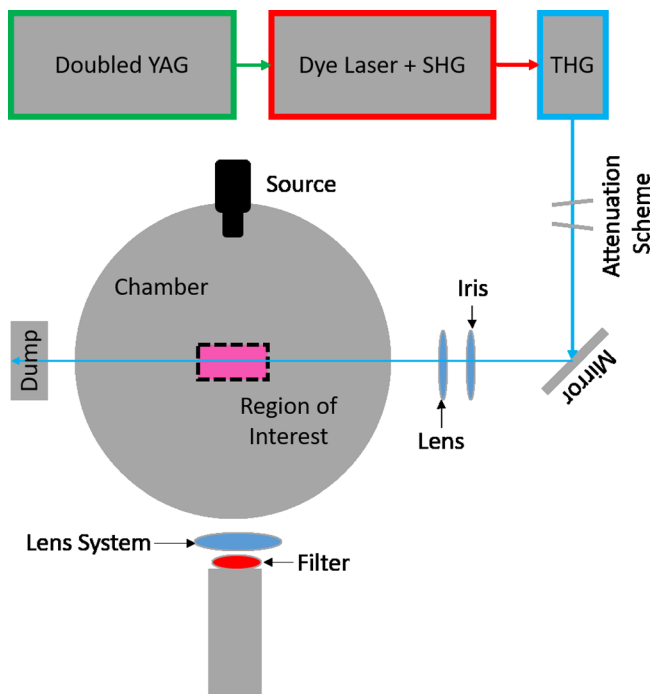


FIG. 1. Schematic representation of the experimental setup (top view).

doubling, through a beta barium borate (BBO) crystal, that is then remixed with residual red light from the dye laser in a second BBO crystal for sum-frequency generation to the required 205 nm radiation; this is then used to conduct two-photon absorption laser induced fluorescence (TALIF). Given the established method,^{14–17} only a brief overview of the methodology will be provided here. The 205 nm radiation is used to excite the ground state hydrogen atoms into the $n = 3$ manifold. Additional complexity can be noted due to the two-photon optical selection rules;¹⁸ ultimately, the outcome through either direct excitation and/or L-state mixing is a fully mixed, but not with an equal ratio, $n = 3$ manifold. In the absence of quenching, this manifold relaxes over a natural time-constant this is referred to as the natural

lifetime. By detecting the fluorescent photons produced during this relaxation, combined with knowledge of the reduced optical branching ratio and various invariant experimental terms, the density of the excited state can be calculated. This excited state density is proportional to the ground state density; however, a calibration using krypton is required to determine absolute ground state densities.^{14,19}

Saturation curve measurements, which are necessary to ensure that no photo-ionization occurs from the excited state, were performed, and an energy per pulse of 370 and 19 μJ was used for hydrogen and krypton, respectively, to avoid this effect. Effective lifetimes were measured to be 12 and 33 ns for hydrogen and krypton, respectively, and were found to be independent of any parametric variation performed in this study. The measurements were conducted at the same vertical and horizontal positions as a Sairem Aura-Wave electron cyclotron resonance (ECR) plasma source, but with a radial displacement of 115 mm. The plasma source was powered by a Sairem microwave generator that was operated at 2.45 GHz throughout the experiments. The base pressure of the reactor was 4.5×10^{-5} Pa, and working pressures were controlled using a butterfly valve linked to a baratron pressure gauge. The gas flow was controlled using two identical MKS mass flow controllers with a total flow rate of 14 sccm into a chamber with a volume of 80 l. The detection scheme used a Nikon lens system focused onto a small region of interest that was approximately 10 and 2 mm in the horizontal and vertical distances, respectively. The fluorescent photon count is an integrated measurement within this region of interest, with each pixel representing a unique spatial location.²⁰ Immediately before the camera, an Andor iStar DH734x iCCD, a spectral filter, with a bandwidth of 10 nm centered around 656 nm for hydrogen and 825 nm for krypton, was installed to filter for only the fluorescence wavelength.

Figure 2(a) shows the single Gaussian spectral profile; each point is an accumulation of 200 laser pulses, for the plasma produced atomic hydrogen (hereafter referred to as the plasma contribution) in a pure hydrogen plasma operated at 5 Pa for an applied power of 150 W. By contrast, upon the addition of 5000 ppm nitrogen into the otherwise pure hydrogen feed gas, a two Gaussian contribution can clearly be observed, as shown in Fig. 2(b); this is due to the two different populations of atomic hydrogen within the fluorescence signal. The narrower Gaussian is the same contribution, as shown in Fig. 2(a), resulting from the dissociation of hydrogen molecules primarily through electron impact dissociation. However, the second contribution (hereafter

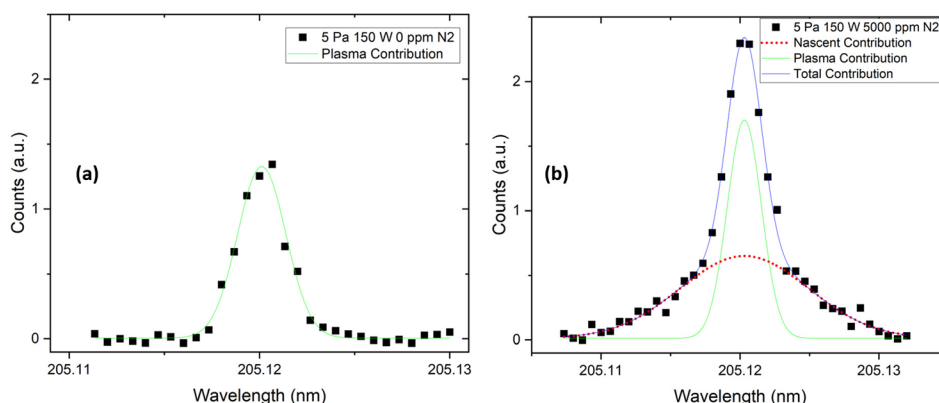


FIG. 2. (a) The Gaussian spectral profile for the $H\alpha$ fluorescence at 656 nm for a pressure of 5 Pa and an applied power of 150 W with 0 ppm nitrogen. Here, a single Gaussian spectral profile can be observed. (b) The same spectral profile with an admixture of 5000 ppm nitrogen. By contrast, a significant deviation from the single Gaussian profile to a double Gaussian structure can be observed; this is due to the creation of a second hydrogen production channel.

referred to as the nascent contribution) is from the detection of a hydrogen atom due to the photolysis of a parent ammonia molecule. The nascent contribution is significantly broader than the plasma contribution; this effect has previously been discussed by Amorim *et al.*⁷ who showed, due to the conservation of momentum law, that the nascent hydrogen atom can have a maximum energy of up to 94% of the total translational energy of the parent molecule.

Figure 3 shows the comparison between the plasma and nascent contributions as a function of nitrogen admixture at an applied power of 100 W for three different pressures: (a) 3 Pa, (b) 5 Pa, and (c) 7 Pa. The trends shown for each of these pressures are identical with the nascent contribution being below the detection threshold for nitrogen admixtures of 1000 ppm and below. The plasma contribution remains approximately static for increasing nitrogen admixtures, while the nascent contribution increases. As shown in Fig. 3(a), the nascent contribution is approximately equal to the plasma contribution with a nitrogen admixture of 1500 ppm. However, Figs. 3(b) and 3(c) show that the equivalent contributions are not reached until a nitrogen admixture of 2500 ppm.

The ammonia itself, from which the nascent contribution is derived, is created through interactions at the wall of the vessel. The most commonly accepted theory is the progressive hydrogenation of nitrogen species through successive recombination with hydrogen atoms. This requires that four atoms must be created within the plasma (three for hydrogen and one for nitrogen). By estimating the gas temperature, assumed to be 300 K, dissociation degrees (as defined by Eq. (1) with n_x denoting the atomic density and $2n_{X_2}$ denoting the number of possible atoms from the diatomic parent molecule) between 0.08 and 0.13% were calculated for atomic hydrogen generated from the plasma contribution. The same can then be done for the dissociation degree for atomic nitrogen; however, an additional assumption must be made in this instance. It must be assumed that the nascent contribution is equal to the ammonia density. Unfortunately, this cannot be stated with complete confidence. However, it can be stated that the nascent contribution is the minimum ammonia density present within the plasma because only one nascent hydrogen atom can be photolysed from the ammonia molecule; this is because the 205 nm radiation is unable to satisfy the approximately 7.6 eV requirement for the photolysis of NH_2 .²¹ This does not mean that there are not ammonia molecules that did not undergo photolysis within the region of interest investigated. The dissociation degrees calculated for atomic nitrogen ranged from 43% to 61% and were found to increase with decreasing pressure. This is in reasonably good agreement with the relative contributions measured by Carrasco *et al.*,⁹ although the nitrogen admixture used in their work was set at 10% of the total feed gas. The significant difference in the dissociation degrees for hydrogen and nitrogen can only be explained by a highly efficient recombination of atomic nitrogen to ammonia at the walls of the chamber,

$$DD = \frac{n_x}{2n_{X_2}} \times 100. \quad (1)$$

Figure 4 shows the fractional contribution of the nascent signal with respect to the total signal as a function of nitrogen admixture for three different pressures: 3, 5, and 7 Pa at an applied power of 100 W. Increasing the pressure decreases the fractional contribution of the nascent signal. However, this becomes less prevalent at higher nitrogen

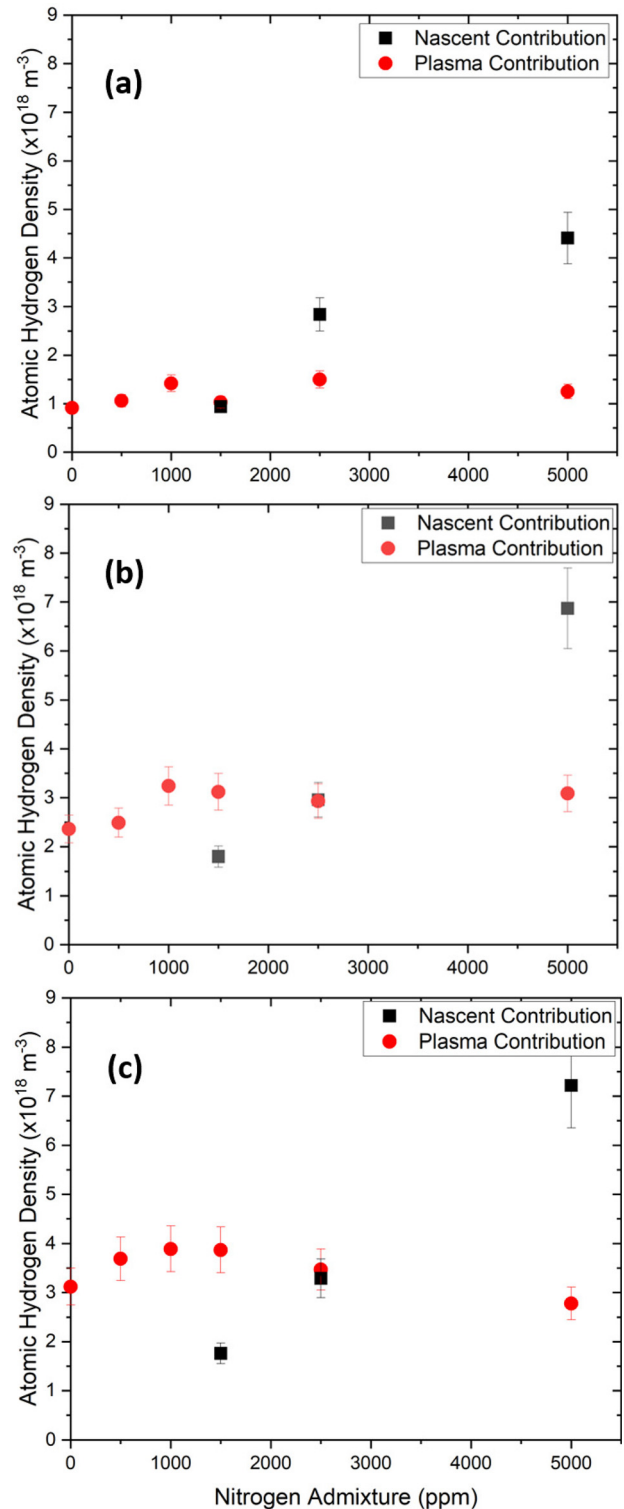


FIG. 3. The plasma and the nascent contributions as a function of nitrogen admixture for a power of 100 W. Three different pressures are shown: (a) 3 Pa, (b) 5 Pa, and (c) 7 Pa.

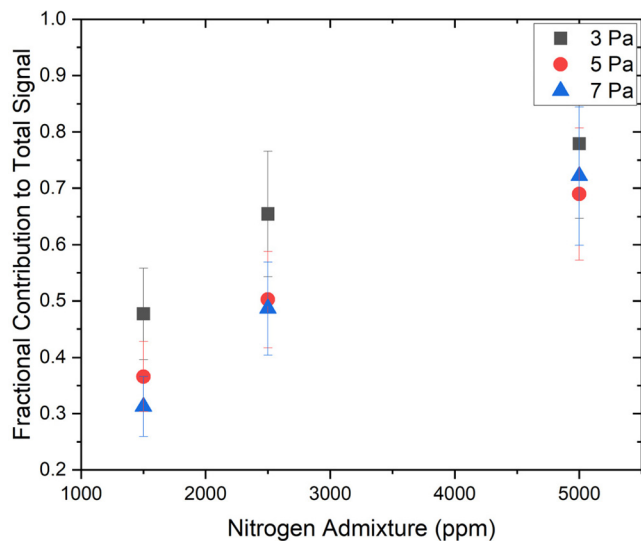


FIG. 4. The fractional contribution, defined as the fraction of the nascent contribution to the total signal as a function of nitrogen admixture for three different pressures.

admixtures. There are two reasons why this may be the case. First, the plasma contribution may simply increase more rapidly than the nascent contribution with increasing pressure. Second, increasing the pressure decreases the diffusion of atoms to the walls as the number of collisions is increased, therefore due to the reliance on atomic diffusion to the walls for the source term, decreasing the production rate of ammonia.

Given the importance of plasma-surface interactions for the production of ammonia, the entire reactor vessel was heated to observe whether a thermal dependency could be detected. Figure 5 shows the

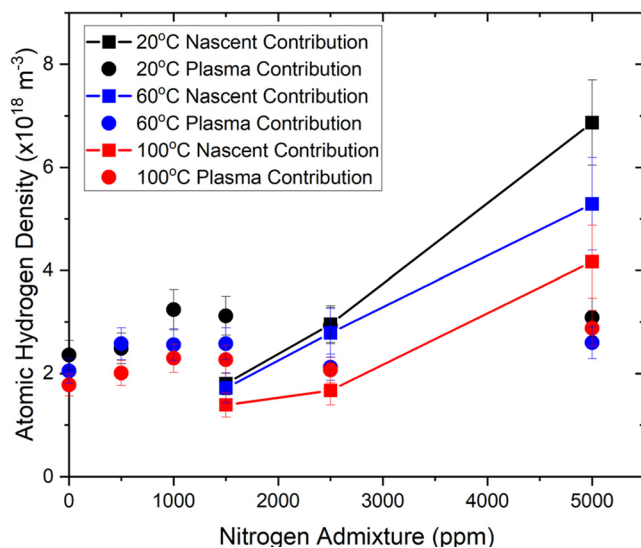


FIG. 5. The plasma and nascent contributions as a function of nitrogen admixture for three different wall temperatures.

comparison between the plasma and nascent contributions as a function of nitrogen admixture for a 5 Pa plasma with an applied power of 100 W. All of the surfaces of the vessel were heated to three different temperatures: 20 °C, 60 °C, and 100 °C. Unfortunately, it is difficult to state with great confidence, due to the large errors involved in performing TALIF, but it appears that the plasma contribution suffers a slight decrease with increasing wall temperature. Nevertheless, the results clearly show that increasing the surface temperature decreases the nascent contribution.

Kim and Boudart²² showed that it is possible to explain the non-trivial temperature dependency of the macroscopic recombination rate by separating the contributions of the LH and ER mechanisms. As further discussed by Cartry *et al.*,²³ the contribution for the LH mechanism increases to a certain threshold value, as the wall temperature is increased so is the atomic thermal energy that subsequently increases the recombination cross section. Moreover, beyond this, it begins to decrease as the characteristic migration distance decreases. By contrast, the ER mechanism increases with increasing temperature until a threshold, approximately 1250 K,²² is reached. Thus, given the observations noted from Fig. 5 of decreasing nascent contribution for increasing wall temperature, the only recombination mechanism to decrease with increasing temperature is the LH mechanism, providing the threshold has been reached and surpassed, and then the dominant mechanism for the creation of ammonia under the conditions investigated in this study must be Langmuir–Hinshelwood. This is in agreement with the simulation work conducted by Carrasco *et al.*,⁹ which found that if the LH mechanism was not accounted for, then a significant discrepancy appears when comparing experimental and simulated data.

It has been shown that a significant amount of ammonia is being created even in a plasma with only very small levels of nitrogen admixed into hydrogen. The nascent contribution, from which the ammonia density is inferred, has been shown to decrease for increasing pressure; one explanation for this is the decreasing flux of atomic nitrogen to the wall with increasing pressure. By combining the nascent hydrogen atom densities with an approximation for the temperature, a dissociation degree has been estimated. A significant discrepancy, a factor of approximately 500, between the dissociation degree of hydrogen and nitrogen has been calculated. We propose that this discrepancy can be explained by a highly effective recombination of atomic nitrogen at the wall to ammonia through progressive hydrogenation of nitrogen and NH_x species. The importance of the wall was shown to be irrefutable by conducting thermal loading experiments; this showed that increasing the temperature of the wall clearly decreases the nascent contribution. This can only be due to the decrease in the Langmuir–Hinshelwood recombination coefficient; from which, it can be inferred that this mechanism is more dominant than the Eley–Rideal mechanism.

AUTHOR DECLARATIONS

Conflict of Interest

The authors have no conflicts to declare.

DATA AVAILABILITY

The data that support the findings of this study are available from the corresponding authors upon reasonable request.

REFERENCES

- ¹A. Puth, L. Kusýn, A. V. Pipa, I. Burlacov, A. Dalke, S. Hamann, J. H. van Helden, H. Biermann, and J. Röpcke, *Plasma Sources Sci. Technol.* **29**, 035001 (2020).
- ²S. Hamann, I. Burlacov, H.-J. Spies, H. Biermann, and J. Röpcke, *J. Appl. Phys.* **121**, 153301 (2017).
- ³T. Body, S. Cousens, J. Kirby, and C. Corr, *Plasma Phys. Controlled Fusion* **60**, 075011 (2018).
- ⁴A. Kallenbach, M. Bernert, R. Dux, L. Casali, T. Eich, L. Giannone, A. Herrmann, R. McDermott, A. Mlynek, H. W. Müller, F. Reimold, J. Schweinzer, M. Sertoli, G. Tardini, W. Treutterer, E. Viezzer, R. Wenninger, M. Wischmeier, and the ASDEX Upgrade Team, *Plasma Phys. Controlled Fusion* **55**, 124041 (2013).
- ⁵E. Carrasco, M. Jiménez-Redondo, I. Tanarro, and V. J. Herrero, *Plasma Phys. Controlled Fusion* **54**, 124019 (2012).
- ⁶K. K. Ostrikov, U. Cvelbar, and A. B. Murphy, *J. Phys. D: Appl. Phys.* **44**, 174001 (2011).
- ⁷J. Amorim, G. Baravian, and G. Sultan, *Appl. Phys. Lett.* **68**, 1915 (1996).
- ⁸J. H. van Helden, W. Wagemans, G. Yagci, R. A. B. Zijlmans, D. C. Schram, R. Engeln, G. Lombardi, G. D. Stancu, and J. Röpcke, *J. Appl. Phys.* **101**, 043305 (2007).
- ⁹E. Carrasco, M. Jiménez-Redondo, I. Tanarro, and V. J. Herrero, *Phys. Chem. Chem. Phys.* **13**, 19561 (2011).
- ¹⁰B. Gordiets, C. M. Ferreira, M. J. Pinheiro, and A. Ricard, *Plasma Sources Sci. Technol.* **7**, 363 (1998).
- ¹¹B. Gordiets, C. M. Ferreira, M. J. Pinheiro, and A. Ricard, *Plasma Sources Sci. Technol.* **7**, 379 (1998).
- ¹²M. Sode, W. Jacob, T. Schwarz-Selinger, and H. Kersten, *J. Appl. Phys.* **117**, 083303 (2015).
- ¹³P. Bletzinger and B. Ganguly, *Chem. Phys. Lett.* **247**, 584 (1995).
- ¹⁴K. Niemi, V. S. v der Gathen, and H. F. Döbele, *J. Phys. D: Appl. Phys.* **34**, 2330 (2001).
- ¹⁵G. D. Stancu, *Plasma Sources Sci. Technol.* **29**, 054001 (2020).
- ¹⁶A. Goehlich, T. Kawetzki, and H. F. Döbele, *J. Chem. Phys.* **108**, 9362 (1998).
- ¹⁷J. Ellis, J. Branson, K. Niemi, E. Wagenaars, and T. Gans, *J. Phys. D: Appl. Phys.* **53**, 485202 (2020).
- ¹⁸B. Preppernau, K. Pearce, A. Tserepi, E. Wurzburg, and T. A. Miller, *Chem. Phys.* **196**, 371 (1995).
- ¹⁹J. B. Schmidt, S. Roy, W. D. Kulatilaka, I. Shkurenkov, I. V. Adamovich, W. R. Lempert, and J. R. Gord, *J. Phys. D: Appl. Phys.* **50**, 015204 (2017).
- ²⁰M. C. Paul and E. E. Scime, *Rev. Sci. Instrum.* **92**, 043532 (2021).
- ²¹R. Vetter, L. Züllicke, A. Koch, E. F. van Dishoeck, and S. D. Peyerimhoff, *J. Chem. Phys.* **104**, 5558 (1996).
- ²²Y. C. Kim and M. Boudart, *Langmuir* **7**, 2999 (1991).
- ²³G. Cartry, L. Magne, and G. Cernogora, *J. Phys. D: Appl. Phys.* **33**, 1303 (2000).